



# Sea Ice

## Part I. Bulk Salinity Versus Ice Floe Thickness

Austin Kovacs

June 1996



**Abstract:** Mathematical expressions have been established for estimating the bulk salinity of Arctic and Antarctic sea ice vs. ice floe thickness. The ice salinity vs. thickness relationships are based on data for over 400 sea ice cores compiled from numerous sources. The results show that the bulk salinity of first-year sea

ice decreases in an exponential trend with ice sheet thickness. A similar trend reoccurs as the winter ice passes through the melt season. The expression for the bulk salinity  $S_b$  in ‰ for first-year sea ice from 10 to 200 cm thick is  $S_b = 4.606 + 91.603/T_f$ , where  $T_f$  is the ice floe thickness in centimeters.

**Cover:** Logging of a sea ice core in the field. After extraction from the ice sheet, the ice core is quickly removed from the ice core barrel and placed on a cutting board, not on the snow, which can draw brine from the ice. The core length is measured. Small holes are then drilled about 2–3 cm deep into the core side at 20-cm increments and a thermistor is inserted in each hole to determine the in-situ temperature of the ice sheet. Closer spaced measurements may be required near the ice sheet surface, top of the ice core, to better define the temperature gradient in the region. The core is next cut into lengths using the cut-off saw, which is mounted at the end of the cutting board, and the axial length of the ice cylinder then is determined (in this case, using a dial gauge measurement jig located beside the notebook). The ice sample is next weighed on an electronic balance and then placed in a sealed plastic bag or container for later melting and salinity measurements. Air and ice sheet temperature, ice porosity and processing time are factors that effect the loss of brine from the ice core during logging. Upward flow of seawater through the permeable ice remaining at the bottom of a borehole will flush brine from the ice. When this ice is finally removed by coring, its brine concentration may have changed appreciably and the subsequent salinity measurement would be in error.

**How to get copies of CRREL technical publications:**

Department of Defense personnel and contractors may order reports through the Defense Technical Information Center:

DTIC-BR SUITE 0944  
8725 JOHN J KINGMAN RD  
FT BELVOIR VA 22060-6218  
Telephone 1 800 225 3842  
E-mail help@dtic.mil  
msorders@dtic.mil  
WWW http://www.dtic.dla.mil/

All others may order reports through the National Technical Information Service:

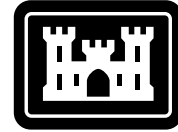
NTIS  
5285 PORT ROYAL RD  
SPRINGFIELD VA 22161  
Telephone 1 703 487 4650  
1 703 487 4639 (TDD for the hearing-impaired)  
E-mail orders@ntis.fedworld.gov  
WWW http://www.fedworld.gov/ntis/ntishome.html

A complete list of all CRREL technical publications is available from:

USACRREL (CECRL-TL)  
72 LYME RD  
HANOVER NH 03755-1290  
Telephone 1 603 646 4338  
E-mail pubs@crrel.usace.army.mil

**For information on all aspects of the Cold Regions Research and Engineering Laboratory, visit our World Wide Web site:  
<http://www.crrel.usace.army.mil>**

CRREL Report 96-7



**US Army Corps  
of Engineers**

Cold Regions Research &  
Engineering Laboratory

# **Sea Ice**

## **Part I. Bulk Salinity Versus Ice Floe Thickness**

Austin Kovacs

June 1996

## **PREFACE**

This report was written by Austin Kovacs, Research Civil Engineer, Applied Research Division, Research and Engineering Directorate, U.S. Army Cold Regions Research and Engineering Laboratory (CRREL), Hanover, New Hampshire.

The author acknowledges, with thanks, Dr. Lewis Shapiro of the University of Alaska and Dr. Donald Perovich of CRREL for their unpublished sea-ice bulk salinity vs. ice sheet thickness data. He thanks Dr. Martin O. Jeffries of the University of Alaska for providing the tabulated ice salinity vs. thickness data from his published figures. The review comments of Dr. Anatoly M. Fish of CRREL, Dr. Walter Spring of Mobil Research and Development Corp., Dr. Wilford F. Weeks of the Geophysical Institute, University of Alaska—Fairbanks, and Dr. Brian Wright of B. Wright and Associates Ltd. are also acknowledged.

The contents of this report are not to be used for advertising or promotional purposes. Citation of brand names does not constitute an official endorsement or approval of the use of such commercial products.

## CONTENTS

	Page
Preface .....	ii
Introduction .....	1
Ice floe brine volume and salinity .....	4
Estimating ice floe salinity .....	6
Summary .....	12
Literature cited .....	13
Abstract .....	17

## ILLUSTRATIONS

### Figure

1. Sea-ice crystal structure .....	1
2. Sea-ice core sections .....	2
3. Over 1-m-long stalactite that formed as a result of cold brine drainage into the sea at the bottom of an ice floe .....	3
4. Three columnar sea-ice crystals with unaligned c-axes .....	3
5. Major 17-cm brine wave migration event observed in Antarctic fast-sea ice .....	4
6. Sea-ice bulk salinity vs. floe thickness as reported by Cox and Weeks .....	5
7. Sea-ice bulk salinity vs. ice sheet thickness and growth time .....	5
8. Sea-ice bulk salinity and growth rate vs. floe thickness .....	6
9. Sea-ice bulk salinity vs. growth time .....	6
10. Comparison of Ryvlin's empirical equation for estimating sea-ice bulk salinity vs. floe thickness .....	7
11. Beaufort Sea first-year ice bulk salinity vs. floe thickness .....	7
12. Sea-ice bulk salinity vs. floe thickness as calculated with Ryvlin's equation for 31.5 and 34‰ seawater .....	8
13. Ryvlin's equation for calculating sea-ice bulk salinity vs. floe thickness where parameter $a$ is constant and varied to match the regression curve through the Beaufort Sea ice data in Figure 11 .....	8
14. Antarctic first-year sea-ice bulk salinity vs. floe thickness data of Jeffries (1994) .....	9
15. Ryvlin's equation for calculating sea-ice bulk salinity vs. floe thickness, where parameter $a$ is constant and varied to match the regression curve through the Antarctic sea-ice data in Figure 14 .....	9

Figure	Page
16. Sea-ice stable salinity and the sea-ice seawater salinity ratio vs. growth rate .....	9
17. Antarctic first-year sea-ice bulk salinity vs. floe thickness data collected from several sources .....	10
18. All Arctic and Antarctic first-year sea-ice bulk salinity vs. floe thickness data compiled from numerous sources .....	10
19. Comparison between the regression curve passed through all the bulk salinity vs. ice floe thickness data in Figure 18 and the field data in Figure 7.....	11
20. Beaufort Sea multiyear ice bulk salinity vs. floe thickness .....	11
21. Beaufort Sea and Antarctic multiyear sea-ice bulk salinity vs. floe thickness .....	12
22. All Arctic and Antarctic multiyear sea-ice bulk salinity vs. floe thickness data .....	12

# Sea Ice

## Part I. Bulk Salinity Versus Ice Floe Thickness

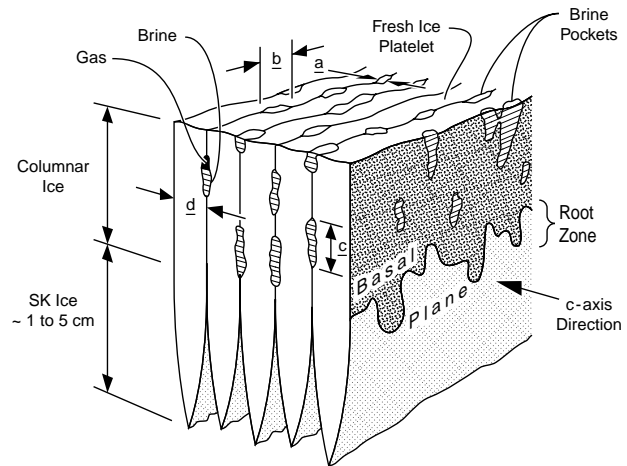
AUSTIN KOVACS

### INTRODUCTION

When seawater freezes, small, flat platelets of fresh ice are first to form. As this ice mass grows, the platelets commingle and bond one to another to form a compliant, highly saline slush called grease ice. With sustained freezing temperatures, the platelet mass thickens and grows together, forming an ever-stiffening ice cover. During this ice growth process most of the seawater is displaced, but between the platelets of pure ice a seawater concentrate called brine becomes entrapped. This entrapment causes the ice to be salty: the salinity of the surface layer of the new ice can be greater than 40‰ (Martin 1979, Kasai and Ono 1984, Ono and Kasai 1985).

Many factors affect the thickness of the platelet or frazil ice layer, including growth rate, sea state, ice pack motion, and under-ice turbulence. However, under relatively quiescent conditions and after the frazil ice layer has "stabilized," the stage is set for the growth of congelation ice. At first, the growing ice platelets, <0.5 mm thick, are randomly oriented, but in time they become more and more ordered, grow wider, and stack one against another. They freeze together in layered groups to form individual ice crystals. Due to thermodynamic factors, preferred platelet growth in seawater is vertical (Weeks and Ackley 1989). Therefore, over a short growth span the ice crystals become "vertically" aligned, with the parallel platelet array having a predominantly horizontal c-axes alignment. The ensuing growth structure is called congelation ice. The number and size of the vertical ice platelets in any crystal vary with growth rate, as does the volume of brine trapped between the fresh-ice platelets (Cox and Weeks 1988, Weeks and Ackley 1989).

Brine entrapment originates in the root area (Fig. 1) of the 1- to 5-cm-thick mushy region called the SK or skeleton layer (Harrison and Tiller 1963) or crystallization front (Cherepanov 1975). In this growth zone the individual ice platelets extend into the seawater, like fingers on a hand, and are typically less than 0.25 mm thick and more than 1 cm wide. As each dendritic platelet grows thicker at its root, it freezes to its neighbor. A high growth rate at this stage (>2 cm/day) results in platelets less than 0.5 mm thick, but at low growth rates (<0.5 cm/day) the platelets can grow to be 1.6 mm thick, with a related increase in crystal size (Weeks and Hamilton 1962a,b; Page 1966; Nakawo and Sinha 1984). During this crystal formation



$$a \leq b < c$$

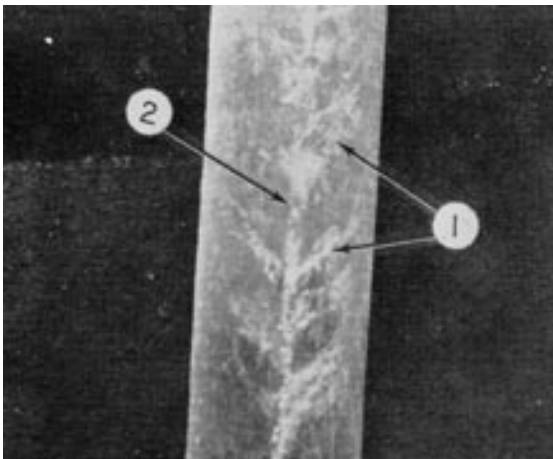
$$a \sim 0.1 \text{ to } 0.3 \text{ mm}; b \sim 1 \text{ to } 5 \times a; c > 5 \times a$$

$$d \sim 0.25 \text{ to } 1.25 \text{ mm (avg } 0.7)$$

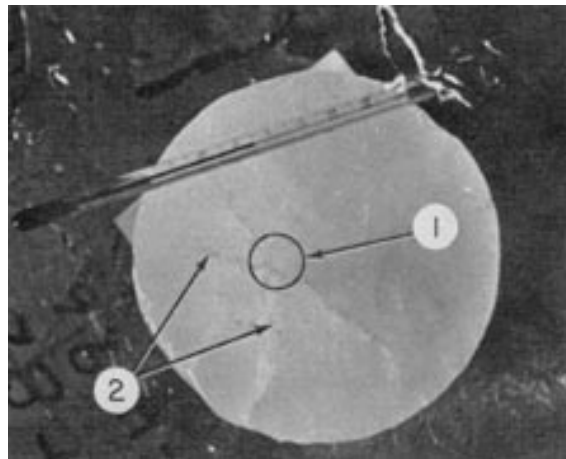
■ Frozen Interface

□ Seawater Interface

Figure 1. Sea-ice crystal structure.



a. Vertical sea ice core showing relative configuration of brine drainage feeder channels (1) extending outward at  $\approx 45^\circ$  from the brine drainage tube (2).



b. Horizontal section across a brine drainage tube. Radiating out from the central brine drainage tube area (1) are numerous brine drainage feeder channels (2).

Figure 2. Sea-ice core sections (from Morey et al. 1984).

process the seawater at the ice growth interface is replaced by supersaturated brine that slows the rate of solidification. As with the frazil/granular surface ice layer, some brine and gas become trapped between the platelets, as depicted in Figure 1. As the ice sheet continues to grow and becomes colder, the film of brine between the ice platelets reduces in volume due to expulsion and drainage processes as well as the freezing out of fresh water from the brine to the surrounding ice surface. The now-isolated brine inclusions are called brine pockets. They are frequently described as ellipsoids, but in fact can have rather complex geometries, depending on ice growth rate and temperature.

Brine expulsion and drainage occur along a flow route that resembles the trunk and branches of a tree, called a drainage tube and channels, respectively. A vertical drainage tube and channel system in Beaufort Sea congelation ice is shown in Figure 2. From 1.5-m-square ice blocks removed from 1- and 1.8-m-thick ice sheets in the Beaufort Sea, I found the drainage tubes at the bottom of the ice to be spaced 5 to 17 cm apart, but they average 10 cm apart. These spacings are in agreement with the findings of Martin (1979), Wakatsuchi (1983), and other investigators. Wakatsuchi also reported that the spatial density of brine tubes depends on the growth rate. The faster the growth rate, the more drainage tubes per unit area. The brine channel inclination varies from  $40^\circ$  to  $54^\circ$ , but averages  $45^\circ$  (Lake and Lewis 1970, Criminale and LeLong 1984).

Brine drainage is high during initial ice formation, but as the ice sheet thickens and becomes

colder, brine flow decreases and much of the drainage system is transformed into a series of brine and gas cells separated by necks of ice (Doronin and Kheisin 1975). The salinity at any given depth now decreases slowly during the remainder of the growth season. Drainage systems form again during the melt season (Nakawo and Sinha 1981). Near-freezing temperatures and solar radiation heating cause melting, "corrosion pockets" form in the ice surface, and internal melting occurs at crystal boundaries, old brine drainage routes, flaws, etc. (Bennington 1967, Cox and Schultz 1980). The corrosion pockets contain liquid with a high salt concentration originating, for example, from the salt residue of the  $>50\%$  salinity brine that was ejected to the surface during initial ice sheet formation (Burke 1940, Zubov 1945, Martin 1979, Drinkwater and Crocker 1988, Perovich and Richter-Menge 1994), from the typically high-salinity frazil or granular ice surface layer (Martin 1979) or from brine concentrated in an ice surface layer formed as a result of ice sheet flooding. The enriched brine then melts into the ice sheet, re-opening or enlarging the old drainage systems as the brine wave descends to the sea. The cold, high-salinity (60 to 70‰) drainage (Lewis and Milne 1977) is followed by increasingly fresher flow resulting from the pure-ice melt or is replaced by an upward flow of less dense seawater (Edie and Martin 1975). Depending on the brine temperature and volume flux and seawater current velocity, on exiting the ice the brine drainage can freeze the seawater around the periphery of the descending brine plume, forming long, delicate, thin-walled hollow ice stalactites (Fig. 3) that





Figure 3. Over 1-m-long stalactite that formed as a result of cold brine drainage into the sea at the bottom of an ice floe.

on occasion can extend up to 6 m below the bottom of the sea ice (Page 1970, Dayton and Martin 1971, Martin 1974, Lewis and Milne 1977, Grishchenko 1988).

As reported in Kovacs and Morey (1980), the growth of congelation sea ice in calm water results in a structure in which the c-axes of the crystals are randomly oriented in the horizontal plane. This is depicted in Figure 4. However, if a current exists under the ice sheet, selective ice

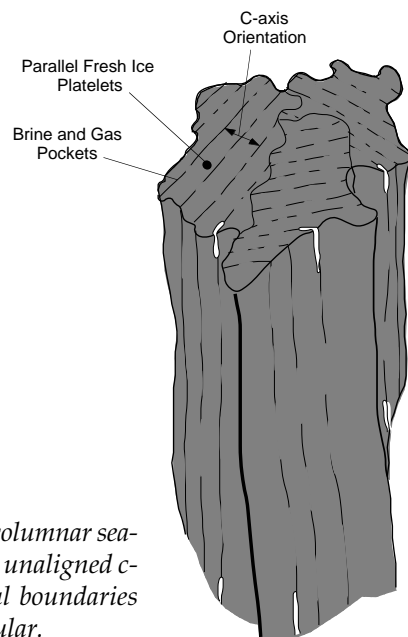


Figure 4. Three columnar sea-ice crystals with unaligned c-axes. The crystal boundaries are highly irregular.

platelet growth and therefore crystal fabric orientation occurs, in which the horizontal c-axes of the ice crystals become aligned with the current (Kovacs and Morey 1978, Weeks and Gow 1978, 1979; Langhorne and Robinson 1986). The significance of this alignment is that it renders the ice sheet horizontally anisotropic, and this in turn affects the electromagnetic (Campbell and Orange 1974; Kovacs and Morey 1978, 1979; Morey et al. 1984) and mechanical (Anderson 1963, Payton 1966, Wang 1979, Timco et al. 1991, Kovacs 1993) properties of the ice. Many other investigators have observed preferred c-axis alignment in sea ice. Perhaps most notable is Cherepanov (1975), who made wide-area sea-ice observations in the seas north of Russia, and, more recently, Gow et al. (1982), who verified that similar sea-ice c-axis alignment occurs in Antarctic congelation sea ice.

While the above description of first-year sea-ice growth does not encompass the many structure variations that can occur due to such factors as snow loading and flooding, thick frazil-ice components (e.g., Cherepanov and Kozlovskiy 1973a,b; Martin 1981; Gow et al. 1987), and large interlaced ice platelet layers, as found, for example, in Antarctic sea ice (e.g., Cherepanov and Kozlovskiy 1973a, Dieckmann et al. 1986, Eicken and Lange 1989, Jeffries and Weeks 1993), it does reveal that sea ice is a multicomponent material. It is composed of fresh ice, brine, and gas inclusions and solid salt crystals (Sinha 1977, Marion and Grant 1994). The volume of fresh ice is by far

the largest fraction, typically in excess of 95%. Sea ice is classified by age (first-year, second-year, and multiyear) and by morphology (flat, ridge, rafted, etc.). Variations in growth, melt, and deformation processes result in ice formations of complex shape and structure and variable brine and gas content. The sea ice may also contain foreign matter such as sediment (e.g., Barnes et al. 1984, Kempema et al. 1989) and microscopic algae and diatoms (e.g., Sutherland 1852; Wright and Priestley 1922; Usachev 1949; Buinitskii 1965, 1974; and many others more recently).

### ICE FLOE BRINE VOLUME AND SALINITY

A number of factors affect the volume of brine that is initially incorporated into the sea ice. Foremost is the salinity of the seawater, the ice growth rate and structure. Under extreme cold conditions, accelerated growth occurs, and more brine tends to be entrapped in the ice at the bottom of the ice sheet (e.g., Malmgren and Sverdrup 1927, Burke 1940, Zubov 1945, Weeks and Lee 1958, Nakawo and Sinha 1981) and for congelation ice the ice platelets that form each ice crystal are narrower (e.g., Weeks and Hamilton 1962a,b; Page 1966; Nakawo and Sinha 1984). As the ice sheet thickens, the rate of growth slows due to the decreasing rate at which heat is transferred from the bottom of the ice to the atmosphere (Makstas 1984, Maykut 1986). This heat exchange is further reduced with increasing snow cover. The net effect is that less brine entrapment occurs as the ice increases in thickness. Over time, very gradual brine migration occurs toward the warmer seawater (Whitman 1926, Zubov 1945, Kingery and Goodnow 1963, Bennington 1967, Untersteiner 1968, Nakawo and Sinha 1981). An explanation for this continued brine migration is the dissolution of ice by the brine at the warmer bottom end of a brine pocket and a refreezing of water at the colder upper end of the pocket. This migration and associated brine drainage gradually reduce the bulk salinity of the ice from an initial value of as much as 25‰ for ice 5 cm thick to about 5‰ for first-year ice about 2 m thick.

Accelerated brine drainage can occur under warming conditions. The enriched brine from the top of the ice sheet can move downward like a wave slowly descending through the ice sheet. During the descent the general form of the wavelet is preserved, but the amplitude (that is, the

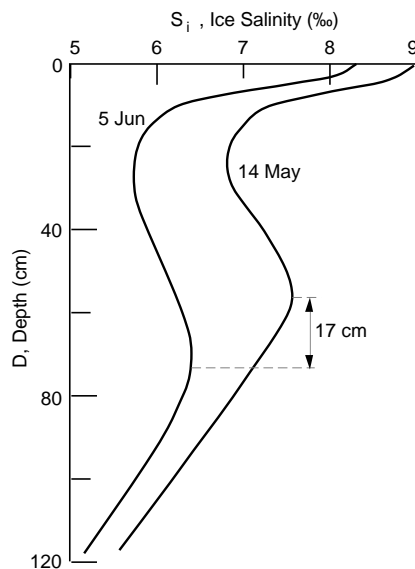


Figure 5. Major 17-cm brine wave migration event observed in Antarctic fast sea ice between 14 May and 5 June (after Doronin and Kheisin 1975).

brine volume) gradually decreases. This is due to brine pockets intercepting the drainage network and draining to the sea in advance of the following brine wave. This drainage phenomenon, illustrated in terms of a very smooth ice sheet salinity distribution profile, is shown in Figure 5. The salinity (brine) migration wave shown is very fast, about 0.8 cm/day. Migration rates one to two orders of magnitude lower may be more typical for winter sea ice, based on the velocity assessments presented by Weeks and Ackley (1989), who give an in-depth review of sea-ice salinity and brine entrapment and migration processes. In addition, it is difficult, at best, to see this movement in the similar data of Nakawo and Sinha (1981), and a rate of 1 mm/day may be estimated from Shapiro and Weeks (1993, Figure 9).

A widely cited study on the bulk salinity variation in sea ice is that of Cox and Weeks (1974). In this study average or bulk salinity data for winter Beaufort Sea ice was collected from a number of sources. Their plot of the salinity vs. ice thickness data clearly shows a decrease in bulk salinity with increasing ice floe thickness (Fig. 6). The available data seemed to justify representing the bulk salinity vs. ice floe thickness trend by the two linear curves shown in Figure 6. However, many natural phenomena tend to follow exponential-like distributions. Sea-ice bulk salinity vs. floe thickness appears to be one of them.

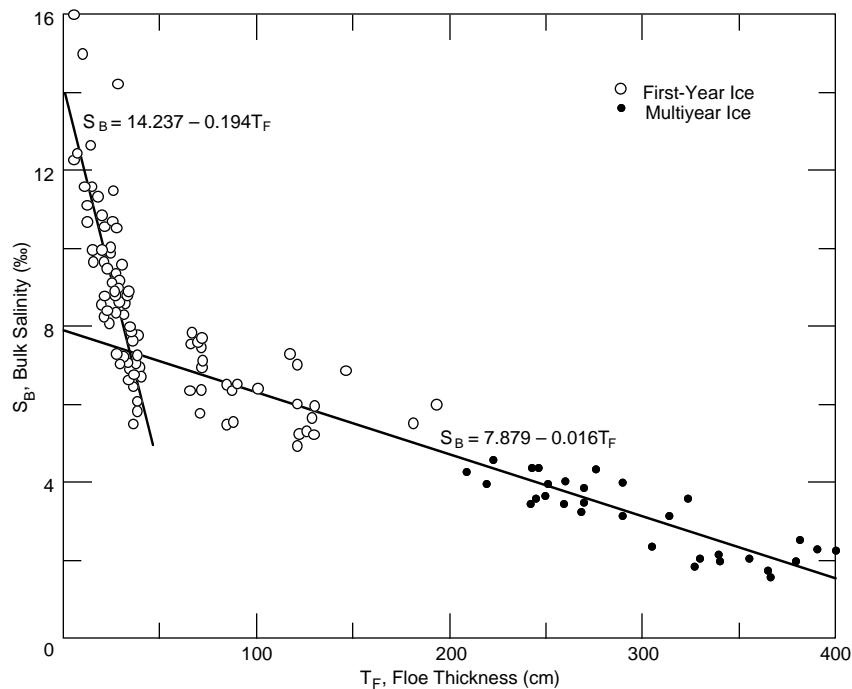


Figure 6. Sea-ice bulk salinity vs. floe thickness as reported by Cox and Weeks (1974).

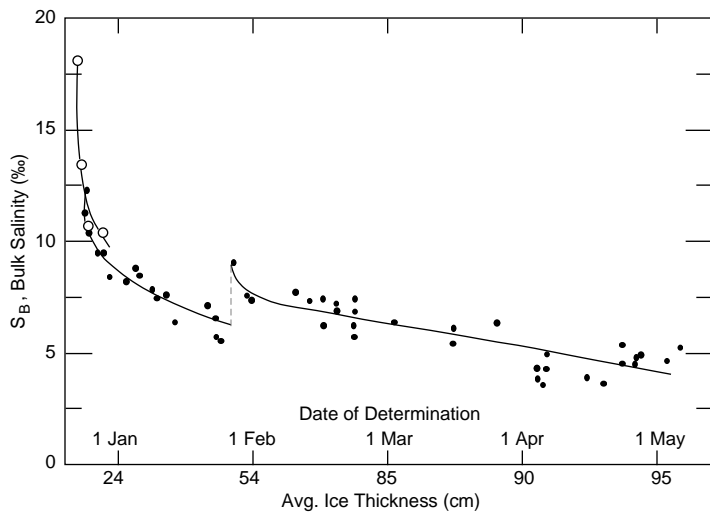


Figure 7. Sea-ice bulk salinity vs. ice sheet thickness and growth time (after Weeks and Lee 1958).

In the mid-1950s, Weeks and Lee (1958) published their observations on the bulk salinity of an ice sheet vs. ice thickness and growth time (Fig. 7). The abrupt step in the curve through the data occurred as a result of a flooding event during which seawater infiltrated the snow cover. Had this not occurred, one could visualize that the trend of the curve before the step would have continued to decrease to a salinity of about 5‰ by May. In any event, the data clearly reveal a

rapid decrease in bulk salinity as the ice sheet grew to about 0.5 m thick and a gradual decrease in bulk salinity thereafter.

Other early reports also confirm that this bulk salinity vs. floe thickness trend applies to Antarctic sea ice. Fedotov (1973) measured the bulk salinity of the fast ice in Alasheev Bight during the growth period. His results are presented in Figure 8. The bulk salinity was found to be about 25‰ in the 5-cm-thick ice but dropped rapidly to about 7.5‰ when the ice was 0.5 m thick. At the end of the measurement period (about 170 days), the ice was 150 cm thick and the bulk salinity had decreased to about 5‰. Doronin and Kheisin (1975) presented results for the bulk salinity of Antarctic

fast sea ice during the growth and melt periods (Fig. 9). This figure again shows a rapid decrease in the bulk salinity during the first growth month, followed by a gradual decrease until the onset of the melt season in October. At this time another rapid decrease in the bulk salinity began, which ended in December. The ice sheet's bulk salinity had by then decreased to about 2‰, a value representative of Arctic multiyear sea ice of similar thickness.

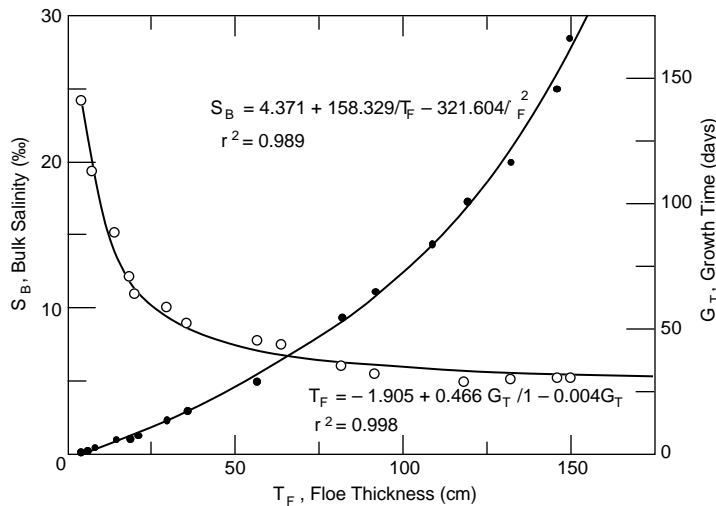


Figure 8. Sea-ice bulk salinity and growth rate vs. floe thickness (after Fedotov 1973).

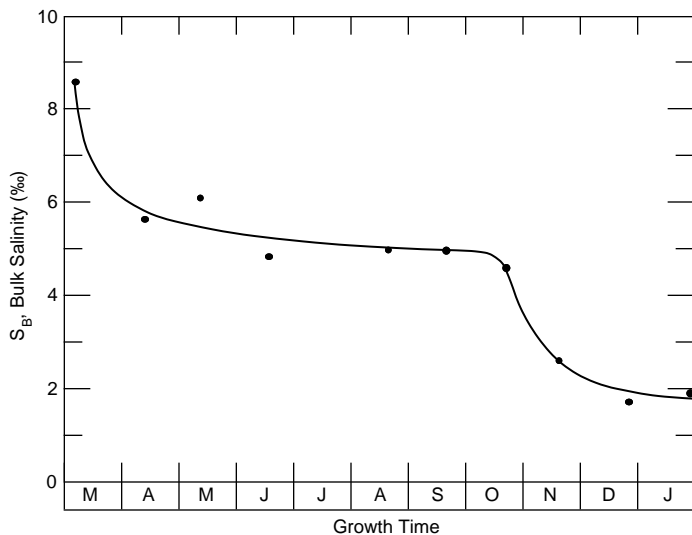


Figure 9. Sea-ice bulk salinity vs. growth time (after Doronin and Kheisin 1975).

The decrease in bulk salinity vs. time shown in Figures 7 and 9 was also observed during laboratory studies of brine entrapment processes in NaCl ice (Cox and Weeks 1975) and in natural sea ice by Fukutomi et al. (1951) and Blinov (1965).

These reports clearly indicate that the bulk salinity of natural and laboratory-grown saline ice decreases rapidly with increasing thickness or time during the early growth phase, followed by a second rapid decrease in the bulk salinity during the early part of the melt season. Because of the latter decrease, the bulk salinity data for “warm” or “old” sea ice should not be combined and analyzed with “cold” first-year sea ice data.

## ESTIMATING ICE FLOE SALINITY

Ryvlin (1974) was one of the first to express the bulk salinity  $S_B$  vs. ice floe thickness  $T_F$  trend empirically. His formula takes into consideration the salinity of the seawater  $S_w$  and the ice sheet growth rate  $G_R$  as follows:

$$S_B = S_w (1 - S_R) e^{-a(T_F)^{0.5}} + S_R S_w \quad (1)$$

where  $S_R = S_{BF}/S_w$  = salinity ratio  
 $S_{BF}$  = final bulk salinity at end of growth season

$a$  = growth rate coefficient, reported to vary from 0.35 to 0.5, e.g., at  $G_R \geq 4$  cm/day,  $a = 0.35$ , and at  $G_R \leq 0.5$  cm/day,  $a = 0.60$ .

Ryvlin suggests that where  $G_R$  is not known, one may assume the value of 0.5 for  $a$ . He also found empirically that  $S_R$  is  $\approx 0.13$ . Using a value of 0.5 and 34‰ for  $a$  and  $S_w$  respectively, and an unknown value for  $S_{BF}$ , Ryvlin compared eq 1 with his and Weeks and Anderson's (1958) first-year sea ice  $S_B$  vs.  $T_F$  field data, as shown in Figure 10. In this comparison, the agreement between the empirical estimate and field measurements is extremely good throughout the entire ice floe thickness range. The question is, does this agreement hold for other data sets?

To evaluate Ryvlin's equation, we first compiled unpublished first-year Beaufort Sea ice  $S_B$  vs.  $T_F$  data that was provided by Perovich (five cores for  $T_F < 25$  cm)

and Kovacs (30 cores), along with published data from Gow and Weeks (two cores, 1977), Tucker et al. (five cores, 1984), and Meese (nine cores, 1989) (Fig. 11). The salinity of the Beaufort Sea near the Alaska coast is 31.5‰. The purpose of using data from just one location is that the salinity of the water is a parameter that affects ice salinity (Weeks and Lofgren 1967, Ryvlin 1974). This can be seen in Figure 12, where the only parameter varied in eq 1 was the seawater salinity. The fixed parameters used in eq 1 to create the curves in Figure 12 were 0.5 for  $a$  and 0.13 for  $S_R$ . For an end-of-growth-season ice thickness of 200 cm,  $S_B$  is 4.44‰ and 4.12‰ for an  $S_w$  of 34‰ and 31.5‰, respectively. For this example, the seawater sa-

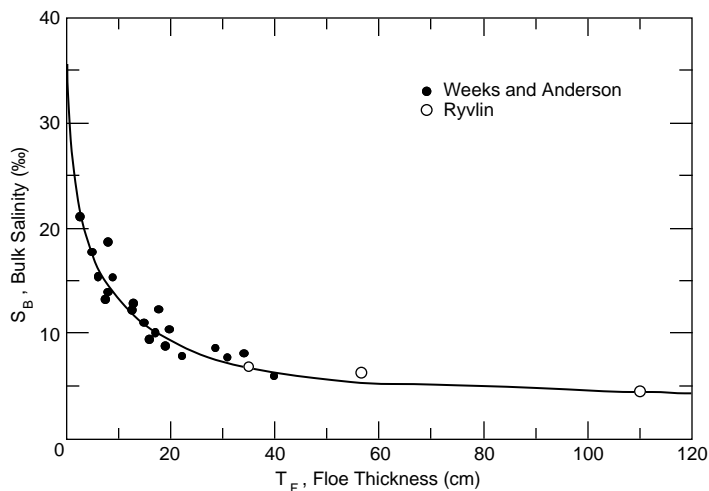


Figure 10. Comparison of Ryvlin's empirical equation for estimating sea-ice bulk salinity vs. floe thickness, with field data (after Ryvlin 1974).

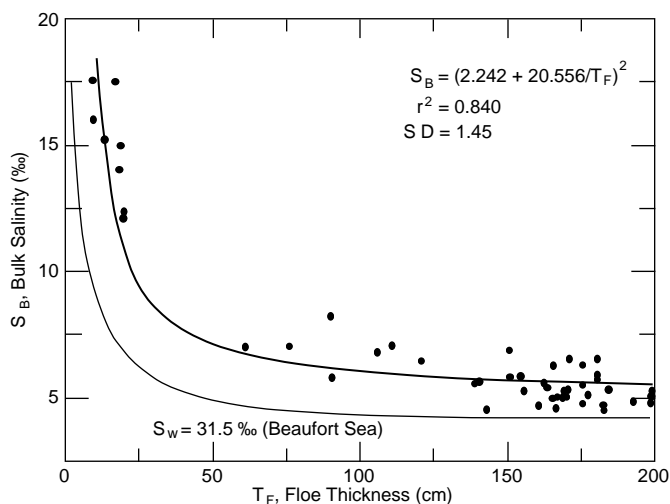


Figure 11. Beaufort Sea first-year ice bulk salinity vs. floe thickness. The lower curve represents the results of Ryvlin's equation for 31.5‰ seawater.

linity difference caused an 8% difference in the bulk sea-ice salinity.

The regression curve through the Beaufort Sea  $S_B$  vs.  $T_F$  data (Fig. 11) is, for all intents and purposes, horizontal after an ice thickness of about 150 cm. Therefore,  $S_{BF}$  may be determined from the regression curve at any  $T_F$  after 150 cm with minor effect on the results of eq 1. For consistency,  $S_{BF}$  at  $T_F = 200$  cm is used in this report.

Running below the regression line, and most of the data, in Figure 11 is the curve derived using eq 1 and an  $S_w$  of 31.5‰ (Fig. 12). Even though the number of data points is limited (and non-existent for a  $T_F$  of 25 to 50 cm) it is apparent that

eq 1 does not fit the data. This is surprising, given the good agreement shown in Figure 10.

At 200 cm the regression curve in Figure 11 gives a value of 5.50‰ for  $S_B$ . Dividing this salinity by  $S_w = 31.5$ ‰ gives a value for  $S_R$  of 0.175, not 0.13 as Ryvlin determined from his data analysis. Using this new  $S_R$  value along with his suggested growth rate coefficient of 0.5 in eq 1 brings the Ryvlin curve into good agreement with the regression curve between  $T_F = 125$  and 200 cm. However, there is still a significant difference between eq 1 and the regression curve where  $T_F$  is less than about 50 cm. To bring the two curves into agreement, coefficient  $a$  has to vary with  $T_F$ . This is shown in Figure 13, where the lower curve represents eq 1 with only  $S_R$  changed from 0.13 to 0.175 and the upper curve represents both the regression line through the data in Figure 11 and eq 1 with  $S_R = 0.175$  and coefficient  $a$  varied as shown.

To verify the need to vary  $S_R$  and  $a$  in eq 1, I analyzed the  $S_B$  vs.  $T_F$  data collected by Jeffries (1994) in the Amundsen and Bellingshausen Seas, Antarctica, in late winter. Unlike the predominantly congelation sea-ice data from the Arctic (Beaufort Sea) the Antarctic sea-ice data are from ice sheets having a predominantly frazil, large interlaced platelet and infiltrated snow ice structure. Core data on ice up to 200 cm thick with a mean temperature below  $-3^\circ\text{C}$  were selected. The latter ensured that the ice was "cold" and not melting. Their data from 74 ice cores are shown in Figure 14. The representative regression curve through the data is of the same form as the one through the Beaufort Sea ice data in

Figure 11. It is important to note that the regression curve at  $T_F = 200$  cm gives  $S_B = 5.41$  vs. 5.50‰ for the Beaufort Sea data. Given the fact that the Antarctic seawater salinity is 34‰\* vs. 31.5‰ for the southern Beaufort Sea, one would expect these  $S_B$  values to be reversed for reasons previously discussed. This unexpected result suggests that the sea-ice data for the

\* M. Jeffries (1995), Geophysical Institute, University of Alaska, Fairbanks, and S. Jacobs (1995), Lamont-Doherty Geological Observatory of Columbia University, Palisades, New York, personal communications.

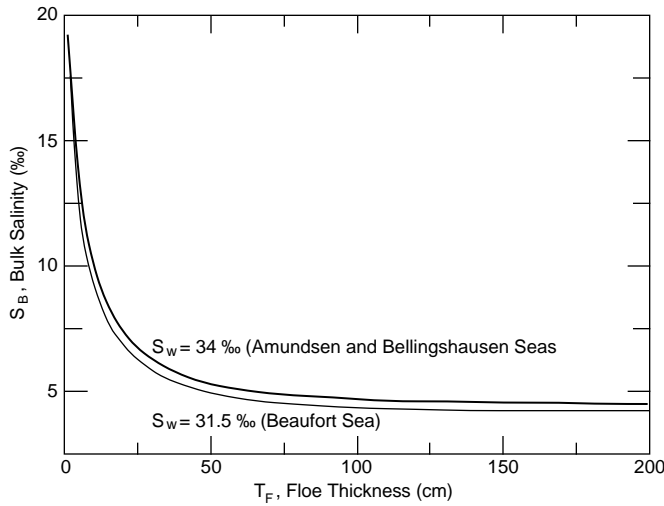


Figure 12. Sea-ice bulk salinity vs. floe thickness as calculated with Ryvlin's equation for 31.5 and 34‰ seawater.

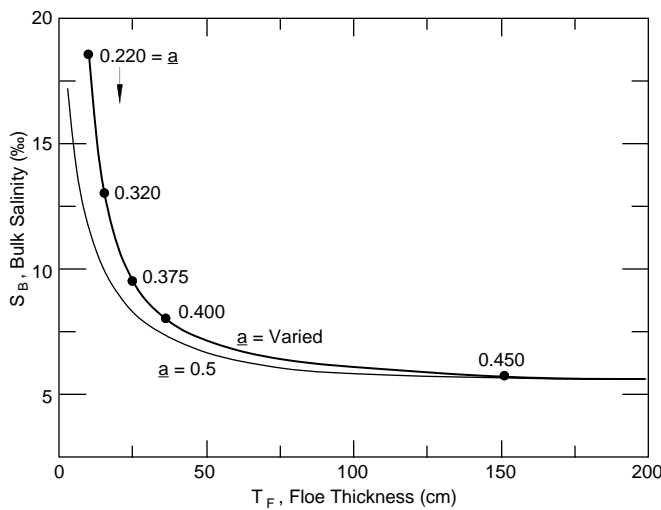


Figure 13. Ryvlin's equation for calculating sea-ice bulk salinity vs. floe thickness where parameter  $\underline{a}$  is constant (lower curve) and varied (upper curve) to match the regression curve through the Beaufort Sea ice data in Figure 11.

Arctic (Fig. 11) and Antarctic (Fig. 14) are not sufficient to fully define the  $S_B$  vs.  $T_F$  trends or that the effect of the seawater salinity difference on  $S_B$  is masked by the scatter in the data and/or ice structure differences. Perhaps as important is the regression curve selected to represent the data. Statistically, two regression curves may fit the data with nearly the same correlation coefficient  $r^2$  value, but they give different  $S_B$  values at 200 cm. In any event, since the regression curves (Fig. 11 and 14) lie well within each other's standard deviation, there is no statistically significant difference between them. Given this reasoning, it would seem that the Arctic and Antarctic sea ice  $S_B$  vs.  $T_F$  data can be combined.

Also shown in Figure 14 is the curve derived from unmodified eq 1 (Fig. 12). As with the Beaufort Sea data, the curve does not fit the data. Taking the regression curve (Fig. 14) value for

$S_{BF} = 5.41\%$  at  $T_F = 200$  and dividing this salinity by  $S_w = 34\%$  gives an  $S_R$  of 0.159. Using this value in eq 1 gives the lower curve in Figure 15. Varying coefficient  $\underline{a}$  at the  $T_F$  increments shown in Figure 15 causes the Ryvlin equation to give  $S_B$  vs.  $T_F$  values that match the regression curve through the Antarctic data (Fig. 14). Both the modified Ryvlin and regression curves are represented by the upper curve in Figure 15.

The fact that growth rate coefficient  $\underline{a}$  needs to vary with  $T_F$  is not surprising. Ryvlin indicated as much in his description of  $\underline{a}$  in eq 1. A further indication of the need to vary  $\underline{a}$  can be seen in Figure 8. Here the time to grow successive increments of ice is shown to increase with thickness. In short, the heat flux through growing sea ice decreases exponentially with thickness and likewise reduces the rate of ice growth (Makshtas 1984, Maykut 1986) and brine entrapment. The

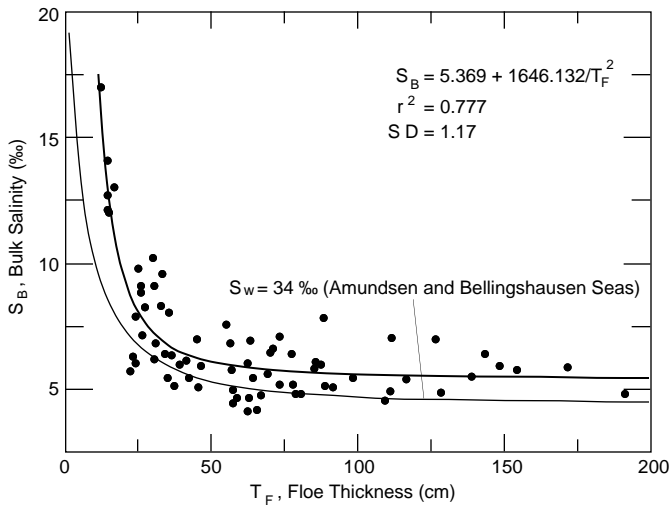


Figure 14. Antarctic first-year sea-ice bulk salinity vs. floe thickness data of Jeffries (1994). The upper curve is the regression fit to the data. The lower curve represents the results using Ryolin's equation for ice grown in 34‰ seawater.

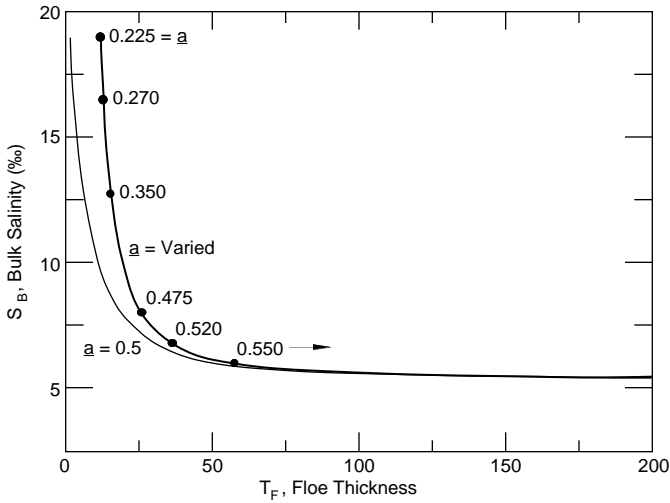


Figure 15. Ryolin's equation for calculating sea-ice bulk salinity vs. floe thickness, where parameter  $a$  is constant (lower curve) and varied (upper curve) to match the regression curve through the Antarctic sea-ice data in Figure 14.

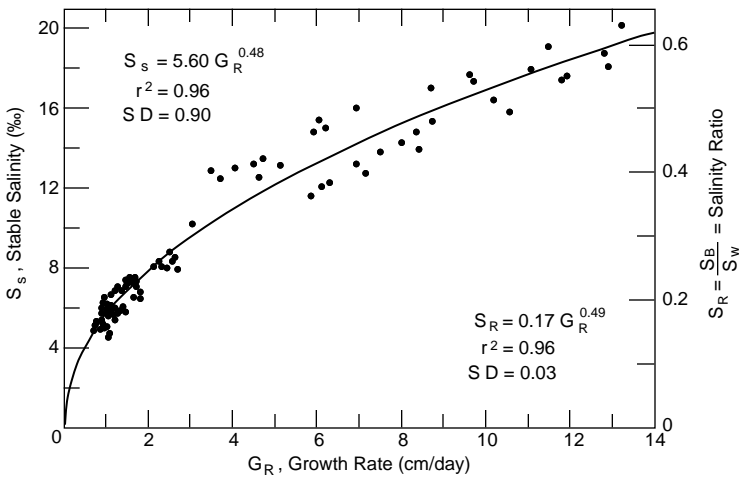


Figure 16. Sea-ice stable salinity and the sea-ice seawater salinity ratio vs. growth rate.

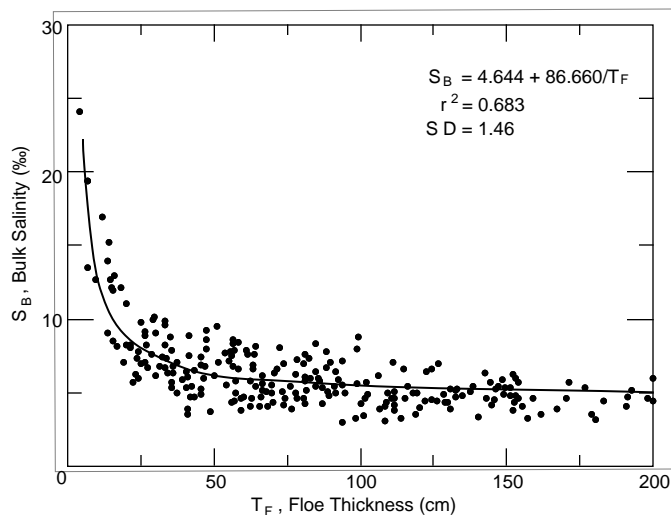


Figure 17. Antarctic first-year sea-ice bulk salinity vs. floe thickness data collected from several sources.

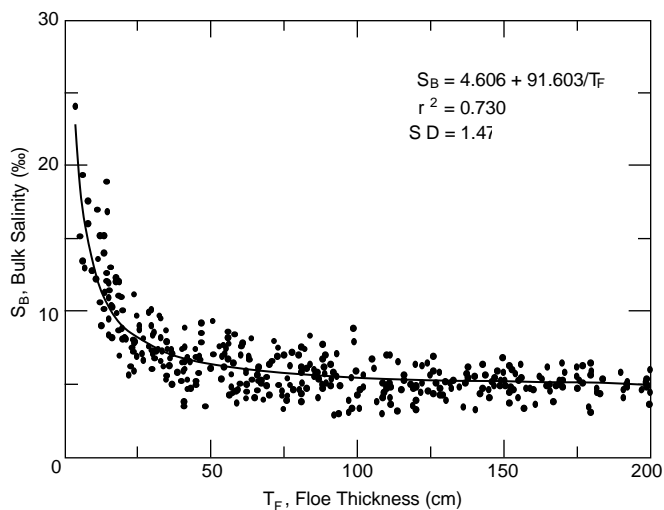


Figure 18. All Arctic and Antarctic first-year sea-ice bulk salinity vs. floe thickness data compiled from numerous sources.

latter, of course, affects the salinity of the ice. This is illustrated in Figure 16, which shows the stable salinity of sea ice vs. growth rate. The data, from measurements made on Arctic and Antarctic sea ice (Nakawo and Sinha 1981, Wakatsuchi 1983), clearly reveal that the salinity of sea ice decreases exponentially with decreasing growth rate. Therefore, the growth rate coefficient for natural sea ice is not a constant, but varies with ice thickness. The scale on the right side of Figure 16 shows the salinity ratio of the ice vs. growth rate. As expected, this ratio is not a constant, but also varies with ice salinity.

In Figure 14 only the Antarctic sea ice data of Jeffries (1994) were used, to eliminate any varia-

tions in sampling techniques that may exist between different research groups and to ensure that the ice sampled grew in seawater of the same salinity. In the comparison between this data set and the Beaufort Sea data, it was found that the effect of seawater salinity on ice salinity was not statistically discernible. Therefore, it seems reasonable to combine the Antarctic  $S_B$  vs.  $T_F$  data of Jeffries (1994) with the Antarctic data of Fedotov (1973), Wakatsuchi (1983), Gow et al. (1987), Makshtas (1984), Eicken (1992), Gow et al. (1992), Ackley et al. (1993), and Veazey et al. (1994). These data, 315 points, are plotted in Figure 17. There is considerable scatter in the data, which can be due to a number of factors: natural growth rate variations (Fig. 16), brine drainage during coring and processing, errors in salinity determination, variations in ice type (infiltrated snow, frazil, platelet and columnar ice), and morphology, such as layered rafted ice. The salinity errors could arise from errors in measuring the ice-core temperature and melt conductivity, measurements that are required for calculating ice salinity. The regression curve through the data in Figure 17 probably gives a better assessment of Antarctic sea ice  $S_B$  vs.  $T_F$  than the curve in Figure 14 because of the increase in the number of data points from 74 to 315.

Combining now the data in Figure 17 with the Arctic data in Figure 11 along with first-year sea ice  $S_B$  vs.  $T_F$  data collected at Thule, Greenland, and Hopedale, Labrador (Weeks and Anderson 1958), Fram Strait (Gow et al. 1987), Port Clarence, Alaska (Kovacs and Kalafut 1977), and Elson Lagoon, Pt. Barrow, Alaska (L.H. Shapiro\* 1994, personal contribution, eight measurements), the distribution shown in Figure 18 is obtained. Interestingly, the regression curve through the combined data gives nearly the same  $S_B$  vs.  $T_F$  values as the curve in Figure 17. For example, at 200 cm both equations give 5.07‰ for  $S_B$ , while at 15 cm the difference is only 0.30‰. This is well within experimental error, and suggests that for most purposes the bulk salinity vs. thickness of undeformed first-year sea ice grown in Arctic and Antarctic seawater with a salinity of about 31 to 34‰ will be very similar. Refinements and standardization of sampling techniques may one day allow us to see the

\* Geophysical Institute, University of Alaska, Fairbanks.



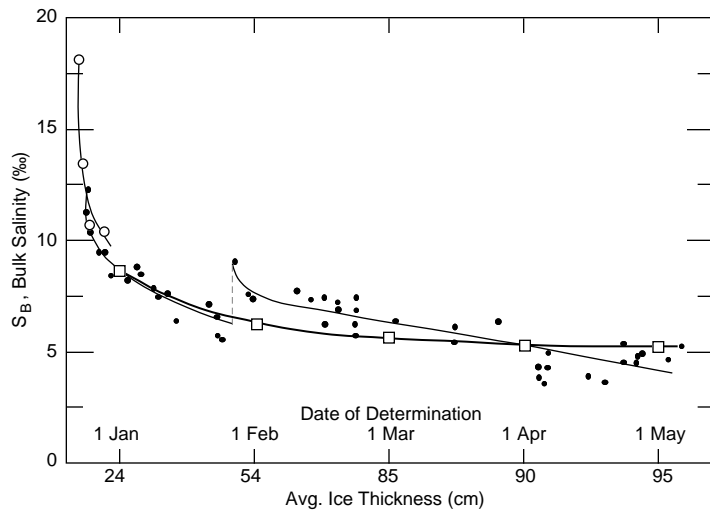


Figure 19. Comparison between the regression curve passed through all the bulk salinity vs. ice floe thickness data in Figure 18 and the field data in Figure 7. The squares mark the locations of the ice thicknesses used in the regression equation given in Figure 18.

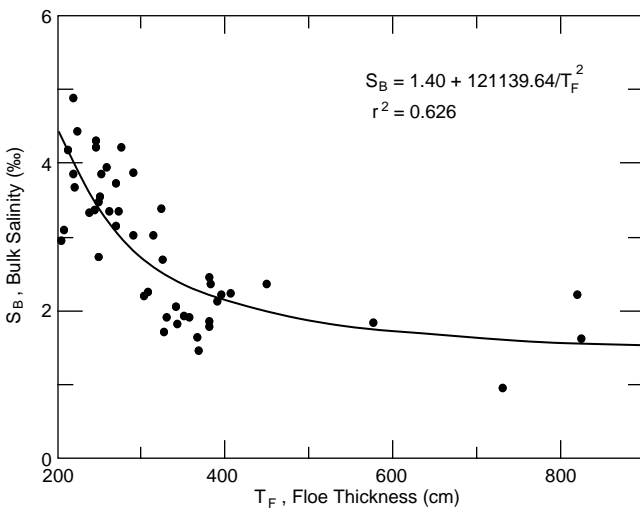


Figure 20. Beaufort Sea multiyear ice bulk salinity vs. floe thickness.

effect of seawater salinity variation as well as first-year sea ice morphology and structure differences on the bulk salinity of the ice. The literature certainly shows that this can be done under controlled conditions (Cox and Weeks 1975, Weeks and Lofgren 1967) and during focused field measurement programs where the highly variable thermodynamic conditions controlling sea ice growth are measured and accounted for (e.g., Nakawo and Sinha 1981, 1984; Wakatsuchi 1983; Eicken 1992). In the interim, Figure 18 provides a good indication of the bulk salinity of first-year sea ice vs. thickness.

It may be of interest now to see how the regression curve in Figure 18 fits the data in Figure 7. Using the five ice thicknesses given in Figure 7 and the equation in Figure 18, the bulk ice sheet salinity was calculated. These values are shown

as boxes in Figure 19 with an interconnecting curve. The agreement is good, considering that ice sheet flooding in January affected ice growth and morphology.

The results in Figure 18 are representative of first-year sea ice during the growth season. In the melt season, ice salinity decreases due to accelerated brine drainage and flushing. Disregarding impurity effects, the speed and intensity of the melt process are highly dependent on thermodynamic factors such as air temperature, solar radiation intensity, snow cover, and rain, as well as the thickness of the ice. These factors govern how fast meltwater forms on the ice surface and the speed at which solar radiation melts the ice around brine channels, pockets, and flaws to help open up the drainage networks leading to the sea. As indicated in Figure 9, spring melt conditions can cause the bulk salinity of the ice to decrease by 50% in one month. At high latitudes, where summer melting is not as intense, the process of ice freshening is slower. Here, more than one melt season may be required to achieve the reduction in ice salinity shown in Figure 9. In lower latitudes, the melt season is longer and sufficiently intense to completely melt the ice cover. Because the degree of ice freshening in one season is highly variable, the salinity of second-year and older ice also varies, but the trend is decidedly to a lower bulk salinity for older ice.

Bulk salinity vs. second- and multiyear ice floe thickness data collected in the Beaufort Sea by Kovacs and Mellor (1971), Cox (1972\*), Kovacs et

\* Only published as shown in Figure 6.

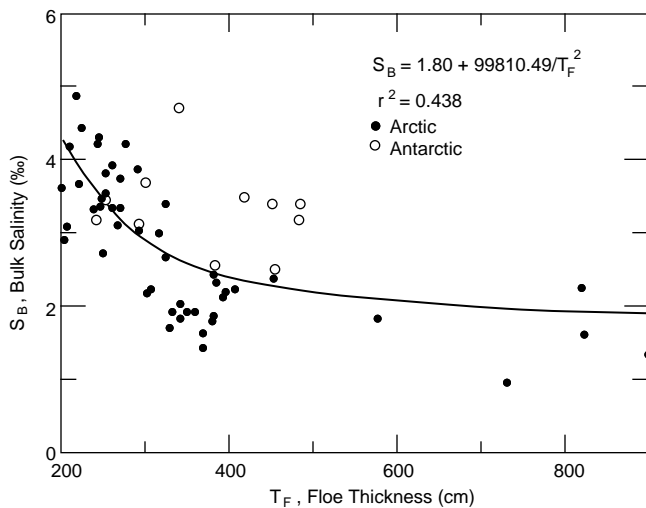


Figure 21. Beaufort Sea and Antarctic multiyear sea-ice bulk salinity vs. floe thickness.

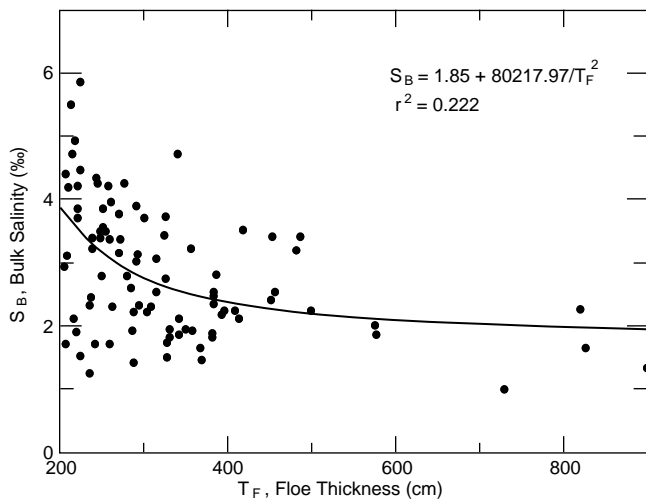


Figure 22. All Arctic and Antarctic multiyear sea-ice bulk salinity vs. floe thickness data.

al. (1973), Cox and Weeks (1974), Kovacs (data on file), and Meese (1989) are shown in Figure 20. The obvious trend is to lower  $S_B$  values with increasing ice thickness.

When the higher  $S_B$  vs.  $T_F$  data for Antarctic multiyear ice (Gow et al. 1987) are added to the Beaufort Sea data the curve through the combined data shifts up slightly for the thicker ice (Fig. 21). The higher Antarctic  $S_B$  values may be due to ice structure, thermodynamic differences during the melt season, or differences in seawater salinity. When the denser brine drains out of the sea ice during the melt season, some of the drainage system can be reoccupied by seawater (Niedrauer and Martin 1979). In the Antarctic, the sea-

water has a higher salinity than in the southern Beaufort Sea. Therefore, the Antarctic sea ice could have a higher salinity due to this possible exchange, if all other parameters are the same.

When multiyear sea ice  $S_B$  vs.  $T_F$  data from Fram Strait (Gow et al. 1987) are added, the distribution changes again, as shown in Figure 22. The scatter in the data between 200 and 300 cm also increases. Some of the lower salinity values from Fram Strait could have resulted from sampling lower-salinity melt-pool ice. Whatever the reason for the lower  $S_B$  values, Figure 22 does indicate that sea ice that has survived one or more melt seasons can freshen to where the bulk salinity is 1 to 2‰.

## SUMMARY

Sea ice salinity data collected in Arctic and Antarctic waters indicate that the bulk ice-sheet salinity decreases with increasing ice floe thickness following a negative exponential-like trend. New ice about 0.05 m thick has a bulk salinity of about 25‰. The bulk salinity of the ice decreases rapidly to about 6‰ at an ice thickness of about 0.5 m. After this, the bulk ice salinity continues to decrease, but at a highly reduced rate, to about 5‰ at the end of the growth season for ice more than 1.5 m thick. Reasons for the salinity decrease are related to ice structure, rate of ice growth, and brine migration processes. The first and second reasons are related, in that as the ice thickness increases, the growth rate slows because the heat exchange from the ice bottom to the atmosphere is reduced. Slower growth results in the formation of larger freshwater ice platelets and larger ice crystals with proportionately fewer brine inclusions. Thus, the ice salinity is lower. Brine migration processes lead to the gradual drainage of brine from the ice to the sea and a freshening of the ice.

Significant scatter and a paucity of data precluded establishing a definitive relationship between seawater salinity and ice sheet structure and the bulk salinity of the sea ice.

A significant decrease in ice floe bulk salinity occurs during the melt season. Depending on many factors, including the solar intensity during the melt season, the bulk salinity of a first-year sea-ice floe can decrease from about 5‰ to about 2‰. This transition to second-year ice separates

the two ice types according to their bulk salinity. For this reason the two ice types' bulk salinity vs. thickness data should not be combined, as previously reported, in an analysis of ice floe salinity–thickness trends.

The Ryvlin relationship for determining the bulk salinity vs. ice floe thickness is difficult, at best, to use since the growth rate parameter is not a constant, but is shown to vary with ice thickness.

The bulk salinity vs. ice floe thickness trend for winter sea ice is well represented by the expression  $S_B = 4.606 + 91.603/T_F$  shown in Figure 18. This expression is applicable to both cold Arctic and Antarctic first-year sea ice grown in seawater of ~31 to 34‰ salinity. The expression should not be used for such southern sea ice environments as the Gulf of St. Lawrence, where winter freeze–thaw cycles are common, and of course the low-salinity Baltic Sea, where ice salinities are typically less than 1‰ for ice as thin as 0.2 m.

#### LITERATURE CITED

- Ackley, S.F., A.J. Gow and V.I. Lytle** (1993) Salinity variations in Weddell Sea pack ice. *Antarctic Journal of the United States*, **28**(5): 79–81.
- Anderson, D.L.** (1963) Use of long-period surface waves for determination of elastic and petrological properties of ice masses. In *Ice and Snow: Properties, Processes and Applications* (W.D. Kingery, Ed.). Cambridge, Massachusetts: MIT Press, p. 63–68.
- Barnes, P.W., D.M. Schell and E. Reimnitz (Eds.)** (1984) *The Alaska Beaufort Sea: Ecosystems and Environments* (various papers). Orlando, Florida: Academic Press.
- Bennington, K.O.** (1967) Desalination features in natural sea ice. *Journal of Glaciology*, **6**(48): 845–857.
- Blinov, L.K.** (1965) Salt content of seawater and ice. *Trudy, Gosudarstvennyy Okeanograficheskiy Institut*, **8**: 5–55, Russian translation, U.S. Naval Oceanographic Office, Washington, D.C., Translation 370.
- Buinitiskii, V.Kh.** (1965) On the influence of diatoms on the structure and strength of sea ice (in Russian). *Problems of the Arctic and Antarctic*, **44**: 83–88.
- Buinitiskii, V.Kh.** (1974) Microscopic algae in Davis Sea fast ice (in Russian). *Problems of the Arctic and Antarctic*, **45**: 100–109.
- Burke, A.K.** (1940) *Morskoe L'dy (Sea Ice)*. Leningrad: Izdatel'stvo Glavsevmorputi. (English translation, Steffanson Collection, Dartmouth College, Hanover, New Hampshire.)
- Campbell, K.J. and A.S. Orange** (1974) The electrical anisotropy of sea ice in the horizontal plane. *Journal of Geophysical Research*, **79**(33): 5059–5063.
- Cherepanov, N.V.** (1975) Main results of an investigation of the crystal structure of sea ice. *Problems of the Arctic and Antarctic*, **41**: 55–68. (English translation, TT 74-52009, National Technical Information Service, U.S. Dept. of Commerce, Springfield, Virginia.)
- Cherepanov, N.V. and A.M. Kozlovskiy** (1973a) Underwater ice in the coastal waters of Antarctica. *Soviet Antarctic Expedition, Information Bulletin*, Bulletin no. 84, American Geophysical Union Translation, **8**(6): 335–338.
- Cherepanov, N.V. and A.M. Kozlovskiy** (1973b) Frazil ice of coastal waters in Antarctica. *Soviet Antarctic Expedition, Information Bulletin*, Bulletin no. 84, American Geophysical Union Translation, **8**(6): 61–65.
- Cox, J.C. and L.A. Schultz** (1980) Brine channel enlargement in sea ice during spring thaw. American Society of Mechanical Engineers, Heat Transfer Division, Publication 80-WA/HT-18: 1–4.
- Cox, G.F.N. and W.F. Weeks** (1974) Salinity variations in sea ice. *Journal of Glaciology*, **13**(67): 109–120.
- Cox, G.F.N. and W.F. Weeks** (1975) Brine drainage and initial salt entrapment in sodium chloride ice. USA Cold Regions Research and Engineering Laboratory, Research Report 345.
- Cox, G.F.N. and W.F. Weeks** (1988) Profile properties of undeformed first-year sea ice. USA Cold Regions Research and Engineering Laboratory, CRREL Report 88-13.
- Criminale, W.O. Jr. and M.-P. LeLong** (1984) Optimum expulsion of brine from sea ice. *Journal of Geophysical Research*, **89**(C3): 3581–3585.
- Dayton, P.K. and S. Martin** (1971) Observations of ice stalactites in McMurdo Sound, Antarctica. *Journal of Geophysical Research, Oceans and Atmospheres*, **76**(6): 1595–1599.
- Dieckmann, G., G. Rohardt, H. Hellmer and J. Kipfstuhl** (1986) The occurrence of ice platelets at 250 m depth near the Filchner Ice Shelf and its significance for sea ice biology. *Deep-Sea Research*, **33**(2): 141–148.
- Doronin, Y.P. and D.E. Kheisin** (1975) *Sea Ice*. (Y.U. Kathavate and V.S. Kothekar, Translators, 1977). Faridabad, India: Oxonian Press Pvt. Ltd.
- Drinkwater, M.R. and G.B. Crocker** (1988) Modelling changes in the dielectric and scattering properties of young snow-covered sea ice at GHz frequencies. *Journal of Glaciology*, **34**(118): 274–282.
- Edie, L.I. and S. Martin** (1975) The formation

- of brine drainage features in young sea ice. *Journal of Glaciology*, **14**(70): 137–154.
- Eicken, H.** (1992) Salinity profiles of Antarctic sea ice: Field data and model results. *Journal of Geophysical Research*, **97**(C10): 15545–15557.
- Eicken, H. and M.A. Lange** (1989) Development of properties of sea ice in the coastal regime of southeastern Weddell Sea. *Journal of Geophysical Research*, **94**(C6): 8193–8206.
- Fedotov, V.I.** (1973) Studies of Antarctic fast ice. In *Studies in Ice Physics and Ice Engineering* (G.N. Iakovlev, Ed.), Proceedings Vol. 300, Arctic and Antarctic Scientific Research Institute (English translation, R. Hardin), p. 95–111.
- Fukutomi, T., K. Kusonoki and T. Tabata** (1951) Study of sea ice: On chlorinity of the coastal land ice observed at Abashiri and Monbetsu in Hokkaido. *Low Temperature Science, Series A*(6).
- Gow, A.J. and W.F. Weeks** (1977) The internal structure of fast ice near Narwhal Island, Beaufort Sea, Alaska. USA Cold Regions Research and Engineering Laboratory, CRREL Report 77-29.
- Gow, A.J., W.B. Tucker III and W.F. Weeks** (1987) Physical properties of summer ice in the Fram Strait, June–July 1984. USA Cold Regions Research and Engineering Laboratory, CRREL Report 87-16.
- Gow, A.J., S.F. Ackley, K.R. Buck and K.M. Golden** (1987) Physical and structural characteristics of Weddell Sea pack ice. USA Cold Regions Research and Engineering Laboratory, CRREL Report 87-14.
- Gow, A.J., S.F. Ackley, V.I. Lytle and D. Bell** (1992) Ice-core studies in the western Weddell Sea (Nathaniel B. Palmer 92-2). *Antarctic Journal of the United States*, **27**(5): 89–90.
- Gow, A.J., S.F. Ackley, W.F. Weeks and J.W. Govoni** (1982) Physical and structural characteristics of Antarctic sea ice. *Annals of Glaciology*, **3**: 113–117.
- Grishchenko, V.D.** (1988) Peculiarities of sea ice desalination in winter (in Russian). Arctic and Antarctic Research Institute, *Trudy*, **401**: 55–64.
- Harrison, J.D. and W.A. Tiller** (1963) Controlled freezing of water. In *Ice and Snow: Properties, Processes and Applications* (W.D. Kingery, Ed.). Cambridge, Massachusetts: MIT Press, p. 215–225.
- Jeffries, M.O.** (1994) Late winter sea-ice properties and growth process in the Bellingshausen and Amundsen Seas. *Antarctic Journal of the United States*, **29**(1): 11.
- Jeffries, M.O. and W.F. Weeks** (1993) Structural characteristics and development of sea ice in the western Ross Sea. *Antarctic Science*, **5**(1): 63–75.
- Kasai, T. and Ono, N.** (1984) An experimental study of brine upward migration in thin sea ice (in Japanese with English summary). *Low Temperature Science, Series A*, **43**: 149–155.
- Kempema, E.W., E. Reimnitz and P.W. Barnes** (1989) Sea ice sediment entrainment and rafting in the Arctic. *Journal of Sediment Petrology*, **59**(2): 308–317.
- Kingery, W.D. and W.H. Goodnow** (1963) Brine migration in salt ice. In *Ice and Snow Properties, Processes and Applications* (W.D. Kingery, Ed.), Cambridge, Massachusetts: MIT Press, p. 237–247.
- Kovacs, A.** (1993) Axial double-ball test versus the uniaxial unconfined compression test for measuring the compressive strength of fresh and sea ice. USA Cold Regions Research and Engineering Laboratory, CRREL Report 93-25.
- Kovacs, A. and J. Kalafut** (1977) Brazil tensile strength tests on sea ice: Data report. USA Cold Regions Research and Engineering Laboratory, Special Report 77-24.
- Kovacs, A. and M. Mellor** (1971) Sea ice pressure ridges and ice islands. Hanover, New Hampshire: Create Science and Technology, Technical Note TN-122.
- Kovacs, A. and R.M. Morey** (1978) Radar anisotropy of sea ice due to preferred azimuthal orientation of the horizontal c-axes of ice crystals. *Journal of Geophysical Research*, **83**(C2): 6037–6046.
- Kovacs, A. and R.M. Morey** (1979) Anisotropic properties of sea ice in the 50–150 MHz range. *Journal of Geophysical Research*, **84**(C9): 5749–5759.
- Kovacs, A. and R.M. Morey** (1980) Investigations of sea ice anisotropy, electromagnetic properties, strength and under-ice current orientation. USA Cold Regions Research and Engineering Laboratory, CRREL Report 80-20.
- Kovacs, A., W.F. Weeks, S. Ackley and W.D. Hibler III** (1973) Structure of a multi-year pressure ridge. *Arctic*, **26**(1): 22–31.
- Lake, R.A. and E.L. Lewis** (1970) Salt rejection by sea ice during growth. *Journal of Geophysical Research*, **75**(3): 583–597.
- Langhorne, P.J. and W.H. Robinson** (1986) Alignment of crystals in sea ice due to fluid motion. *Cold Regions Science and Technology*, **12**(2): 197–214.
- Lewis, E.L. and A.R. Milne** (1977) Underwater sea ice formations. In *Proceedings of the Polar Oceans Conference, May 1974, Montreal, Canada* (M.J. Dunbar, Ed.). Arctic Institute of North America, p. 239–245.
- Makshatas, A.P.** (1984) The heat balance of Arctic ice in winter. Leningrad: Gidrometeoizdat. (English translation, International Glaciological Society, Cambridge, U.K., 1991).
- Malmgren, F. and H.U. Sverdrup** (1927) On the

- properties of sea ice. In *The Norwegian North Polar Expedition with the "Maud," 1918–1929, Scientific Results*, **1**(5): 1–67. Bergen: Geofysisk Institutt.
- Marion, G.M. and S.A. Grant** (1994) FREZCHEM: A chemical–thermodynamic model for aqueous solutions at subzero temperatures. USA Cold Regions Research and Engineering Laboratory, Special Report 94-18.
- Martin, S.** (1974) Ice stalactites: Comparison of a laminar flow theory with experiment. *Journal of Fluid Mechanics*, **63**(1): 51–79.
- Martin, S.** (1979) A field study of brine drainage and oil entrainment in first-year sea ice. *Journal of Glaciology*, **22**(88): 473–502.
- Martin, S.** (1981) Frazil ice in rivers and oceans. *Annual Review of Fluid Mechanics*, **13**: 379–397.
- Maykut, G.A.** (1986) The surface heat and mass balance. In *The Geophysics of Sea Ice* (N. Untersteiner, Ed.). New York: Plenum Press, p. 395–463.
- Meese, D.A.** (1989) The chemical and structural properties of sea ice in the southern Beaufort Sea. USA Cold Regions Research and Engineering Laboratory, CRREL Report 89-25.
- Morey, R.M., A. Kovacs and G.F.N. Cox** (1984) Electromagnetic properties of sea ice. *Cold Regions Science and Technology*, **9**(1): 53–75.
- Nakawo, M. and N.K. Sinha** (1981) Growth rate and salinity profile of first-year sea ice in the high Arctic. *Journal of Glaciology*, **27**(96): 315–330.
- Nakawo, M. and N.K. Sinha** (1984) A note on brine layer spacing of first-year sea ice. *Atmosphere–Ocean*, **22**(2): 193–206.
- Niedrauer, T.M. and S. Martin** (1979) An experimental study of brine drainage and convection in young sea ice. *Journal of Geophysical Research*, **84**(C3): 1176–1186.
- Ono, N. and T. Kasai** (1985) Surface layer salinity of young sea ice. In *Proceedings of the Symposium on Snow and Ice Processes at the Earth's Surface, 2–7 September, 1984, Sapporo, Japan*, *Annals of Glaciology*, **6**: 298–299.
- Page, R.A.** (1966) Crystallographic studies of sea ice in McMurdo Sound, Antarctica. U.S. Naval Civil Engineering Laboratory, NCEL Report R-494.
- Page, R.A.** (1970) Stalactite growth beneath sea ice. *Science*, **167**: 171.
- Payton, H.R.** (1966) Sea ice strength. Geophysical Institute, University of Alaska, Report UAG-182.
- Perovich, D.K. and J.A. Richter-Menge** (1994) Surface characteristics of lead ice. *Journal of Geophysical Research*, **99**(C8): 16341–16350.
- Ryvlin, A.Ia.** (1974) Method of forecasting flexural strength of an ice cover (in Russian). *Problems of the Arctic and Antarctic*, **45**: 79–86.
- Shapiro, L.H. and W.F. Weeks** (1993) Influence of crystallographic and structural properties on the flexural strength of small sea ice beams. In *Ice Mechanics* (J.P. Dempsey, Z.P. Baezant, Y.D.S. Rajapakse and S.S. Sunder, Eds.), AMD–Vol. 163, Book no. G00786. New York: American Society of Mechanical Engineers, p. 177–188.
- Sinha, N.K.** (1977) Technique for studying structure of sea ice. *Journal of Glaciology*, **18**(79): 315–323.
- Sutherland, P.C.** (1852) *Journal of a voyage in Baffin's Bay and Barrow Straits, in the years 1850–1851 performed by H.M. ships Lady Franklin and Sophia, under the command of Mr. William Penney, in search of the missing crews of H.M. ships Erebus and Terror*. London: Longman, Brown, Green and Longmans.
- Timko, G.W., R.M.W. Frederking, S.J. Jones, R.F. McKenna, J. Tillotson and I.J. Jordan** (Eds.) (1991) Seasonal compressive strength of Beaufort Sea ice sheets. In *Ice–Structure Interaction, Proceedings of the IUTAM/IAHR Symposium, St. John's, Newfoundland, 1989*. Berlin: Springer-Verlag, p. 267–282.
- Tucker, W.B. III, A.J. Gow and J.A. Richter** (1984) On small-scale horizontal variations of salinity in first-year sea ice. *Journal of Geophysical Research*, **89**(C4): 6505–6514.
- Untersteiner, N.** (1968) Natural desalination and equilibrium salinity profile of perennial sea ice. *Journal of Geophysical Research*, **73**(4): 1251–1257.
- Usachev, P.I.** (1949) The microflora of polar ice (in Russian). *Trudy Instituta Okeanologii*, **3**: 216–259.
- Veazey, A.L., M.O. Jeffries and K. Morris** (1994) Small-scale variability of physical properties and structural characteristics of Antarctic fast ice. In *Proceedings of the 5th International Symposium on Antarctic Glaciology (VISAG), 5–11 September, Cambridge, U.K.* (E.M. Morris, Ed.), *Annals of Glaciology*, **20**: 61–66.
- Wakatsuchi, M.** (1983) Brine exclusion process from growing sea ice. Contribution–Hokkaido University (Sapporo). *Low Temperature Science, Series A*, no. 33, p. 29–65.
- Wang, Y.S.** (1979) Sea ice properties. In *Technical Seminar on Alaskan Beaufort Sea Gravel Island Design, Houston, Texas*. Production Research Co.
- Weeks, W.F. and S.F. Ackley** (1989) The growth, structure and properties of sea ice. In *The Geophysics of Sea Ice* (N. Untersteiner, Ed.). New York and London: Plenum Press, p. 9–164.
- Weeks, W.F. and D.L. Anderson** (1958) An experimental study of strength of young sea ice. *Transactions of the American Geophysical Union*, **39**(4): 641–647.
- Weeks, W.F. and A.J. Gow** (1978) Preferred crys-

tal orientation in the fast-ice along the margins of the Arctic Ocean. *Journal of Geophysical Research*, **83**(C10): 5105–5121.

**Weeks, W.F. and A.J. Gow** (1979) Crystal alignments in the fast ice of arctic Alaska. USA Cold Regions Research and Engineering Laboratory, CRREL Report 79-22.

**Weeks, W.F. and W.L. Hamilton** (1962a) Petrographic characteristics of young sea ice, Point Barrow, Alaska. *American Mineralogist*, **47**(7–8): 945–961.

**Weeks, W.F. and W.L. Hamilton** (1962b) Petrographic characteristics of young sea ice, Point Barrow, Alaska. USA Cold Regions Research and Engineering Laboratory, Research Report 101.

**Weeks, W.F. and O.S. Lee** (1958) Observations on

the physical properties of sea ice at Hopedale, Labrador. *Arctic*, **11**(3): 135–155.

**Weeks, W.F. and G. Lofgren** (1967) The effective solute distribution coefficient during freezing of NaCl solutions. In *Physics of Snow and Ice, Proceedings of the International Conference on Low Temperature Science, Sapporo, Japan*, (H. Oura, Ed.), **1**(1): 579–597.

**Whitman, W.G.** (1926) The elimination of salt from seawater ice. *American Journal of Science*, **211**: 126–132.

**Wright, C.S. and R.E. Priestley** (1922) *Glaciology, British (Terra Nova) Antarctic Expedition 1910–1913*. London: Harrison and Sons.

**Zubov, N.N.** (1945) *L'dy Arktiki (Arctic Ice)*. Moscow: Izdatel'stvo Glavsevmorputi. (English translation, U.S. Navy Electronics Laboratory.)

